Synthesis, Characterization, Cellular Uptake, and *In Vitro* Anticancer Activity of Fullerenol-Doxorubicin Conjugates

Beihua Xu[1], Li Yuan[2,3], Ying Hu[4], Zhiyuan Xu[2], Jiang-Jiang Qin[1,2]* and Xiang-Dong Cheng[2]*

[1]College of Pharmaceutical Sciences, Zhejiang Chinese Medical University, Hangzhou, China, [2]Institute of Cancer and Basic Medicine, Chinese Academy of Sciences, Cancer Hospital of the University of Chinese Academy of Sciences, Zhejiang Cancer Hospital, Hangzhou, China, [3]First Clinical Medical College, Zhejiang Chinese Medical University, Hangzhou, China, [4]School of Pharmaceutical Sciences, Zhejiang Pharmaceutical College, Ningbo, China

Doxorubicin (DOX) is one of the most commonly used chemotherapeutic agents for treating human cancer. However, its clinical use has been limited by DOX-induced cardiotoxicity as well as other side effects. In the present study, we designed and synthesized the fullerenol (FU)-DOX conjugates and folic acid (FA)-grafted FU-DOX conjugates for improving the selectivity and activity of DOX in cancer cells. We further characterized the physicochemical properties and examined the release kinetics, cellular uptake, and *in vitro* anticancer activities of FU-DOX and FA-FU-DOX. The results showed that FU-DOX and FA-FU-DOX had a mean diameter of <200 nm and a low polydispersity. Both FU-DOX and FA-FU-DOX exhibited pH sensitivity and their DOX release rates were higher at pH 5.9 vs. pH 7.4. The cellular uptake studies indicated that FU conjugation enhanced the intracellular accumulation of DOX in human hepatocellular carcinoma (HCC) cell lines (BEL-7402 and HepG2) and the immortalized normal human hepatocytes (L02). The conjugation of FA to FU-DOX further promoted the drug internalization in an FR-dependent manner and enhanced the cytotoxicity against HCC cells. In conclusion, the newly prepared FA-FU-DOX conjugates can optimize the safety and efficacy profile of DOX.

Keywords: fullerenol-doxorubicin conjugates, cancer, cellular uptake, microscopic imaging, targeted delivery

INTRODUCTION

Doxorubicin (DOX, also named adriamycin), as a broad-spectrum anticancer drug, is widely used in leukemia, lymphomas, and solid tumors such as liver cancer, breast cancer, ovarian cancer, etc. (Kalyanaraman, 2020). However, the side effects of DOX, such as life-threatening cardiotoxicity, hepatotoxicity, and bone marrow suppression limit its clinical application (Gonçalves et al., 2020). The development of drug delivery system is considered as an effective and feasible strategy to enhance the efficacy of chemotherapeutic drugs and reduce its side effects (Raj et al., 2019; Ouyang et al., 2020). In recent years, numerous studies have shown that a variety of nanocarriers can improve the bioavailability and therapeutic efficacy of anticancer drugs while providing preferential accumulation at the target site (Tan et al., 2020). Among them, fullerenes and their derivatives are also attracting more attention for their unique physicochemical properties and biological activities (Kumar and Raza 2018).

Fullerene is a series of cage-like, spherical nano-molecules formed by carbon atoms, which have been found to have some excellent biological activities, such as antioxidant, antiviral, anticancer, and

immunomodulatory effects, etc. (Xu et al., 2011; Martinez et al., 2016; Hao et al., 2017; Xu et al., 2019). Besides, fullerenes have the ability to accumulate in the tumor mass; based on the enhanced permeability and retention (EPR) effect, they penetrate easily through the less-tight blood vessels nourishing cancer (Kepinska et al., 2018a; Kepinska et al., 2018b). In addition, fullerene and hydroxylated fullerene (fullerenol, FU) have also been reported to have the cardioprotective and hepatoprotective effects (Borović et al., 2014; Elshater et al., 2018; Petrovic et al., 2018). The administration of fullerene alone before DOX administration or complexed with DOX via non-covalent bonds could diminish DOX-induced acute toxicity in the heart or liver (Borović et al., 2014; Seke et al., 2016; Jacevic et al., 2019; Petrovic et al., 2018). More importantly, fullerene can act as a transporter for anticancer drugs, such as DOX (Grebinyk et al., 2019; Kazemzadeh and Mozafari, 2019). These biological properties of fullerenes and the potential ability to carry drugs make it attractive to be applied in the drug delivery system.

Tumor targeted drug delivery systems (TTDDSs) can selectively deliver cytotoxic substances to tumor tissues, thus minimizing the side effects of patients and improving the treatment index (Xiao et al., 2020). Folate receptor (FR) has attracted considerable attention in this field. Its expression is limited in normal cells but overexpressed in most tumor cells, such as liver cancer, lung cancer, breast cancer, and so on (Boss and Ametamey, 2020). More importantly, in the receptor-mediated internalization pathway, FR interacts with TTDDSs and rapidly recycles back to the cell surface for the maximum delivery of targeted therapeutics (Fernández et al., 2018). Researchers have grafted folic acid (FA) to the surface of various drug delivery systems, which has significantly increased the drug accumulation in tumors (Su et al., 2020; Tie et al., 2020).

Since cardiotoxicity and hepatotoxicity are the main reasons for restricting the application of DOX, FU with cardioprotective and hepatoprotective effects is increasingly being developed as a drug delivery system for DOX. Several recent studies have indicated that the non-covalent nanocomplex of DOX and fullerene or FU can significantly increase the cytotoxicity of DOX and reduce its side effects on the heart and liver (Seke et al., 2016; Petrovic et al., 2018; Maleki et al., 2020). However, other studies have shown that the loading of DOX onto FU nanoparticles with non-covalent bonds or the conjugated complex of DOX and FU with ester bonds might be unstable in the body and cannot deliver drugs efficiently (Chaudhuri et al., 2009). In the present study, DOX and FU conjugates (FU-DOX) were synthesized by using an acid-sensitive hydrazone bond and further modified by FA to obtain FA-FU-DOX conjugates for improving the tumor-targeting effects. Besides, the cellular uptake and cytotoxicity of FU-DOX and FA-FU-DOX were also examined.

MATERIALS AND METHODS

Materials
Doxorubicin hydrochloride (DOX, also named adriamycin, Shanghai Jizhi Biochemical Technology Co., Ltd.), fullerenol (FU, Suzhou Hengqiu Technology Co., Ltd.), folic acid (FA),

N-hydroxysuccinimide (NHS), N1-((ethylimino)methylene)-N3,N3-dimethylpropane-1,3-diamine (EDC), oxalohydrazide, dimethyl sulfoxide (DMSO), acetic acid, ethanol, methanol, etc. were obtained commercially and used without further purification.

Synthesis of Folic Acid-Grafted Fullerenol-Doxorubicin Conjugates (FA-FU-DOX).

Preparation of Hydrazinated Fullerenol (FU-CONHNH2)
As shown in **Figure 1**, oxalohydrazide (100 mg) was added to a solution of fullerenol (100 mg, 87 μmol) in purified water (10 ml). The reaction mixture was stirred at 50°C for 5 days. Then, it was subjected to dialysis through a cellulose membrane (MW 1000) against deionized water for three times. After 2 days of lyophilization, a dark brown product FU-CONHNH2 was obtained.

Synthesis of Fullerenol-Doxorubicin Conjugates (FU-DOX)
Doxorubicin hydrochloride (30 mg, 50 μmol) and acetic acid (1 drop) as a catalyst were added to the solution of FU-CONHNH2 (70 mg, 50 μmol) in water (10 ml) (**Figure 1**). The reaction solution was stirred for 2 days in the dark at room temperature. When the thin-layer chromatography (TLC) showed little DOX left, the reaction mixture was poured into methanol (30 ml) to precipitate the products. The precipitation was filtrated and washed by methanol three times and dried under reduced pressure to give 58 mg dark red solid with 69% yield.

Preparation of Folic Acid Succinimidyl Ester (FA-NHS)
Folic acid (38 mg, 86 μmol) and DMSO (2 ml) were put into a round bottom flask and sonicated until completely dissolved (**Figure 1**). Then, NHS (11 mg, 95 μmol) and EDC (33 mg, 172 μmol) were added and the reaction mixture was stirred under nitrogen protection in dark at room temperature overnight. An orange-red solution was obtained, which was the activated folic acid (FA-NHS).

Synthesis of Folic Acid-Grafted Fullerenol-Doxorubicin Conjugates (FA-FU-DOX)
The prepared FA-NHS solution (19 mg, 43 μmol, 1 ml) was added into a solution of fullerenol-doxorubicin conjugates (85 mg, 43 μmol) in a mixed solvent of water and DMSO (1: 1) (20 ml). The reaction solution was stirred in dark at room temperature for 8 h (**Figure 1**). The products were precipitated upon treatment with ethanol and filtered to give a brown solid with 64% yield.

Characterization of FA-FU-DOX
Nuclear Magnetic Resonance, Infrared Spectroscopy, and Differential Thermal Analysis
The NMR spectra were recorded on a Bruker advance 500 nuclear magnetic resonance (NMR) spectrometer, using tetramethylsilane (TMS) as an internal reference. D_2O was used as a solvent for fullerenol and deuterated DMSO was used as a solvent for FA,

FIGURE 1 | Reaction route for the synthesis of FA-FU-DOX.
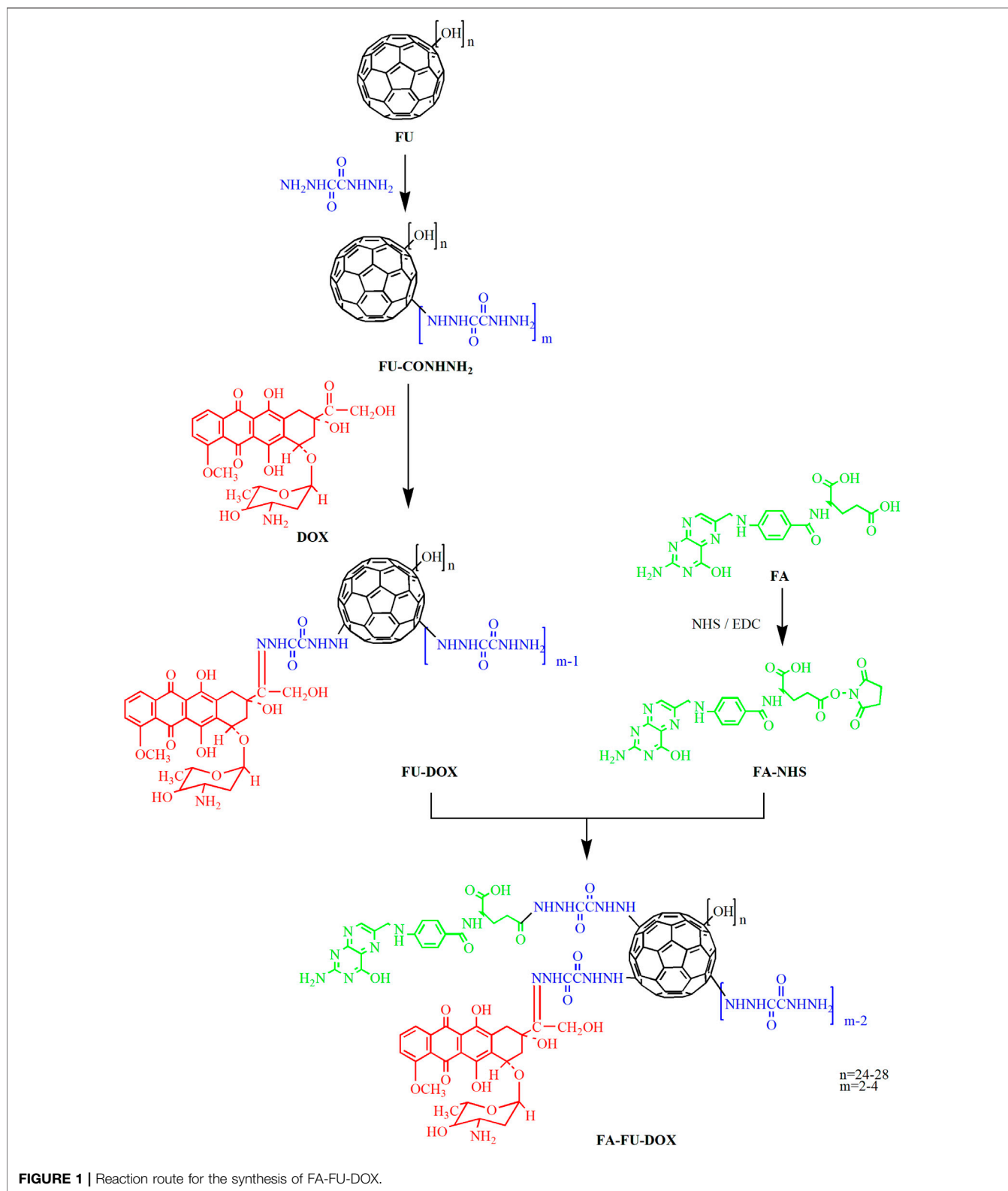
DOX, and FA-FU-DOX. The infrared (IR) spectra were recorded on a Fourier-transform infrared (FTIR) spectrometer (Thermo Fisher Nicolet iS50). KBr tablets of DOX and DOX derivatives were used in the IR instrument. The IR spectra were acquired after 16 scans with a scanning range of 400–4,000 cm^{-1}. Differential thermal analysis (DTA) was done in Mettler Toledo DSC. The detection conditions were 30–300°C, the heating rate was 15°C/min, and the N_2 flow was 100 ml/min.

Transmission Electron Microscope and Dynamic Light Scattering

The diameter and morphology of FU, FU-DOX, and FA-FU-DOX were obtained by a transmission electron microscope (TEM, H-7650, Hitachi, Japan). Dispersions of particles were dropped onto a carbon-coated copper grid, dried in air at room temperature, and imaged immediately. The size distribution of the FU-DOX and FA-FU-DOX complexes was determined by dynamic light scattering (DLS) using Zetasizer Nano ZS-90 (Malvern, United Kingdom). Data were recorded at 25°C with a detection angle of 173° (Voruganti et al., 2015).

Release Kinetic Studies of FU-DOX and FA-FU-DOX

Preparation of a Standardization Curve

To obtain a 100 mg/L stock solution of DOX, the accurately weighed DOX (5.0 mg) was put in a 50 ml volumetric flask, to which DMSO was added to dissolve and dilute to the set volume. To prepare the DOX series solutions with concentrations of 2, 5, 10, 20, and 40 mg/L, 0.2, 0.5, 1.0, 2.0, and 4.0 ml of the stock solutions were added into a 10 ml volumetric flask, diluted with DMSO to a constant volume, and recorded on a UV-2550 spectrophotometer (Shimadzu, Japan). The regression equation
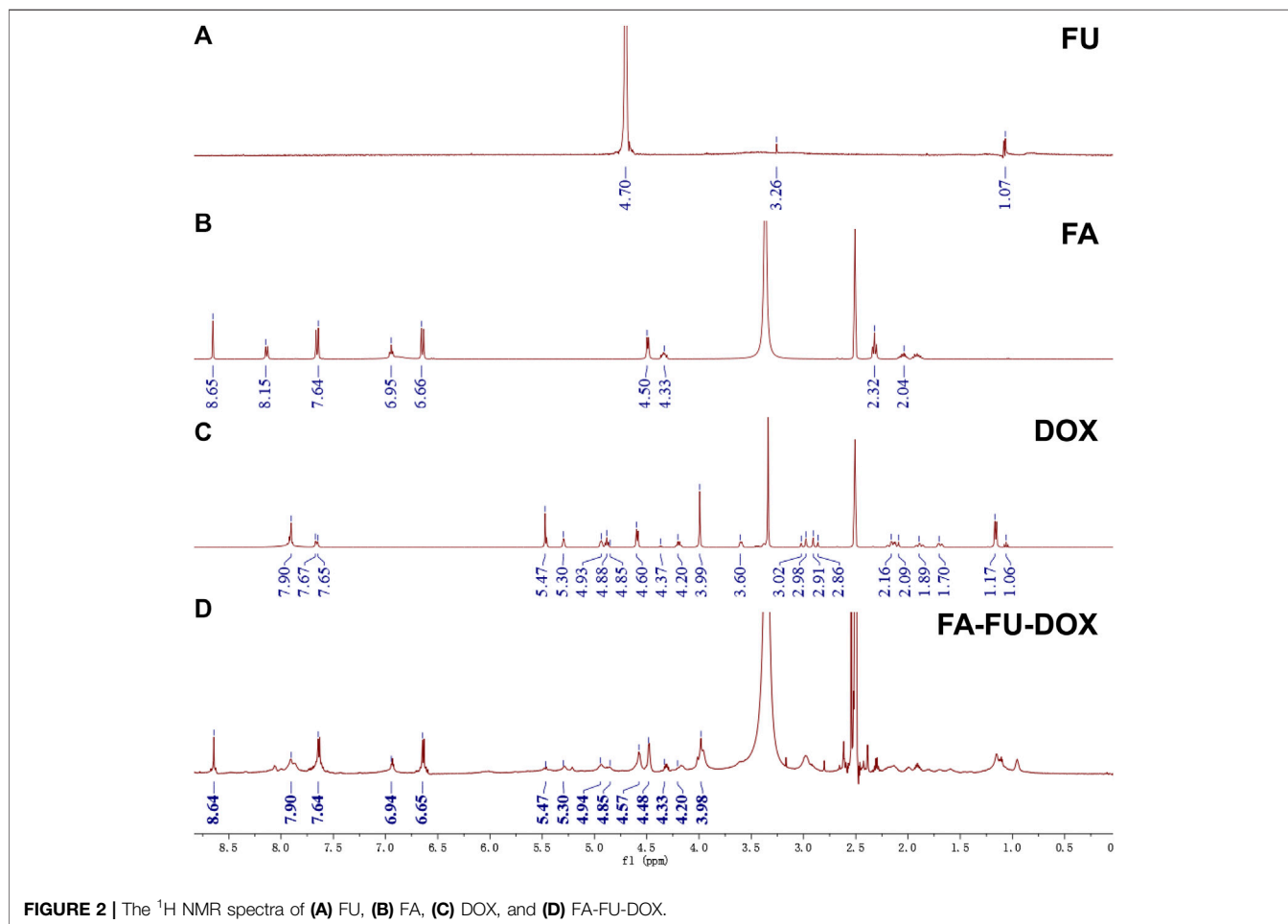
was $A = 0.022C − 0.027$ (r = 0.999), indicating that the peak area of DOX has a good linear relationship within the concentration of 0–40 mg/L region.
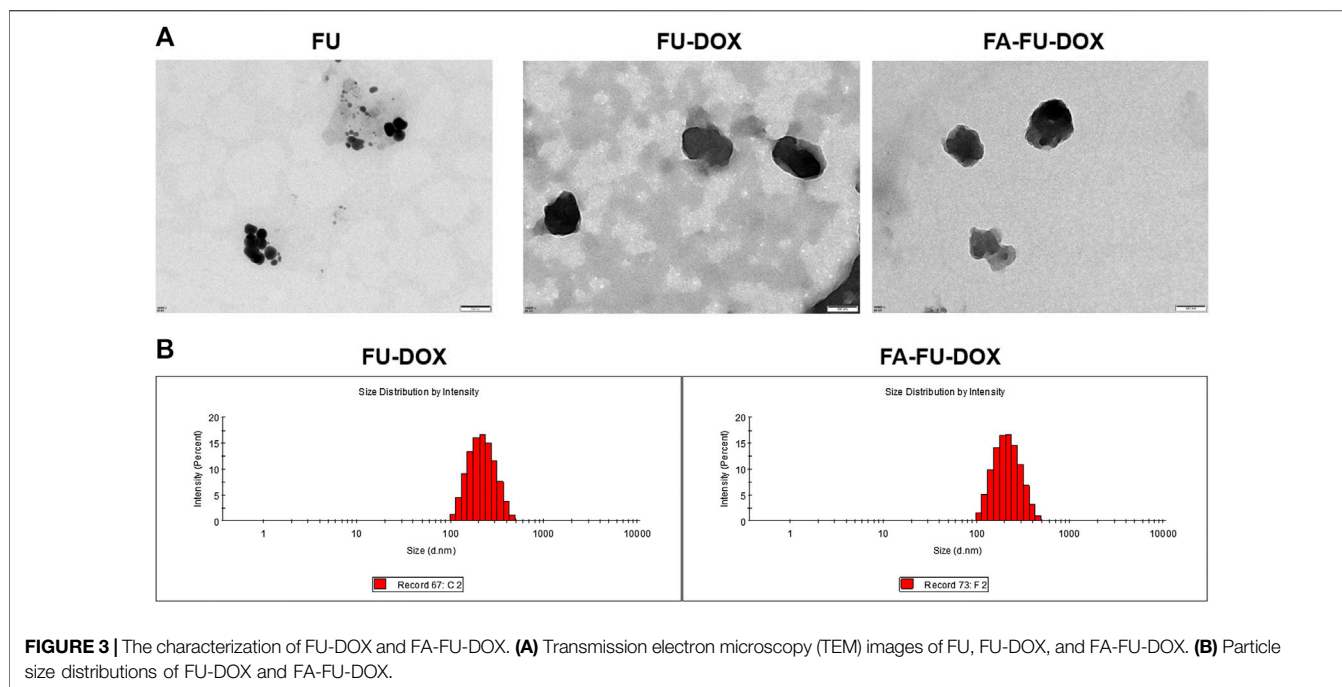
Drug Release Studies

Portions (2.0 mg) of FU-DOX or FA-FU-DOX were put into dialysis bags (MW 1000), which were placed into the releasing medium of phosphate buffer (30 ml) at a pH of 7.4 or 5.9, in vials respectively. The closed vials were then placed in the water bath and incubated at 37°C. The concentration of released DOX was determined by the UV spectrophotometer at predetermined time points. The rate of drug release was calculated by dividing the concentration of DOX (released from FU-DOX or FA-FU-DOX) at a certain time by the initial concentration of FU-DOX or FA-FU-DOX (Voruganti et al., 2015).

Cell Lines and Cell Culture

Human hepatocellular carcinoma (HCC) cell lines (BEL-7402 and HepG2) and the immortalized normal human hepatocytes (L02) were obtained from the Cell Bank of the Chinese Academy of Science (Shanghai, China). All cell lines were cultured in DMEM medium supplemented with 10% fetal bovine serum (FBS) and 1% penicillin/streptomycin as described previously (Wang et al., 2019).

FIGURE 2 | The ^{1}H NMR spectra of **(A)** FU, **(B)** FA, **(C)** DOX, and **(D)** FA-FU-DOX.

FIGURE 3 | The characterization of FU-DOX and FA-FU-DOX. **(A)** Transmission electron microscopy (TEM) images of FU, FU-DOX, and FA-FU-DOX. **(B)** Particle size distributions of FU-DOX and FA-FU-DOX.

Cellular Uptake Studies of DOX, FU-DOX, and FA-FU-DOX

Fluorescence Microscopic Imaging

The cellular uptake of DOX, FU-DOX, and FA-FU-DOX was examined by fluorescence microscopic imaging as reported previously (Qin et al., 2016). In detail, a piece of coverslip was put into each well of 6-well plates. Cells were seeded on the coverslips in 6-well plates at a cell density of 3×10^5 cells/well in 2 ml of culture medium. After 24 h of incubation, cells were treated with DOX, FU-DOX, or FA-FU-DOX at equivalent concentrations of 3 μM DOX. After 1, 2, and 4 h of incubation, the drug-containing medium was discarded. The cells were washed with PBS three times, fixed with 75% ice-cold ethanol for 30 min, and analyzed under a Fluorescence Microscope Axio Observer A1 (Zeiss, German).

Flow Cytometry Analysis

Cells were incubated in 6-well plates (3×10^5 cells/well) for 24 h and then treated with DOX, FU-DOX, or FA-FU-DOX at equivalent concentrations of 3 μM DOX for 1, 2, and 4 h. The treated cells were washed with PBS, harvested, measured by an FACS Calibur flow cytometer (BD, United States), and analyzed with the CytExpert software (Beckman Coulter, United States) (Wang et al., 2020b).

In Vitro Anticancer Activity Evaluation

The cell viability assay was performed as described previously (Wang et al., 2020a; Zhang et al., 2020). Briefly, cells were grown in 96-well plates (3×10^3 cells/well) for 24 h and incubated with DOX, FU-DOX, or FA-FU-DOX at equivalent concentrations for 72 h. Then, 10 μL of CCK-8 solution (Beyotime, CA) was added to each well. The cells were further incubated at 37°C for 2 h and examined by measuring absorption at 450 nm with an MK-3 microplate reader (Thermo Fisher Scientific, United States) (Li et al., 2013; Qin et al., 2013).

Statistical Analysis

All data were generated from three or more independent experiments and presented as means ± SD. The data were analyzed using Student's t-test by Prism software version 6 (Graph Pad Software Inc., United States) and the critical level of significance was set at $p < 0.05$.
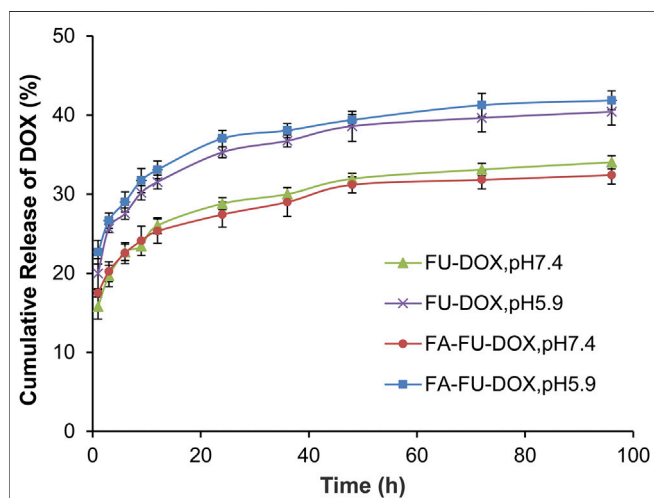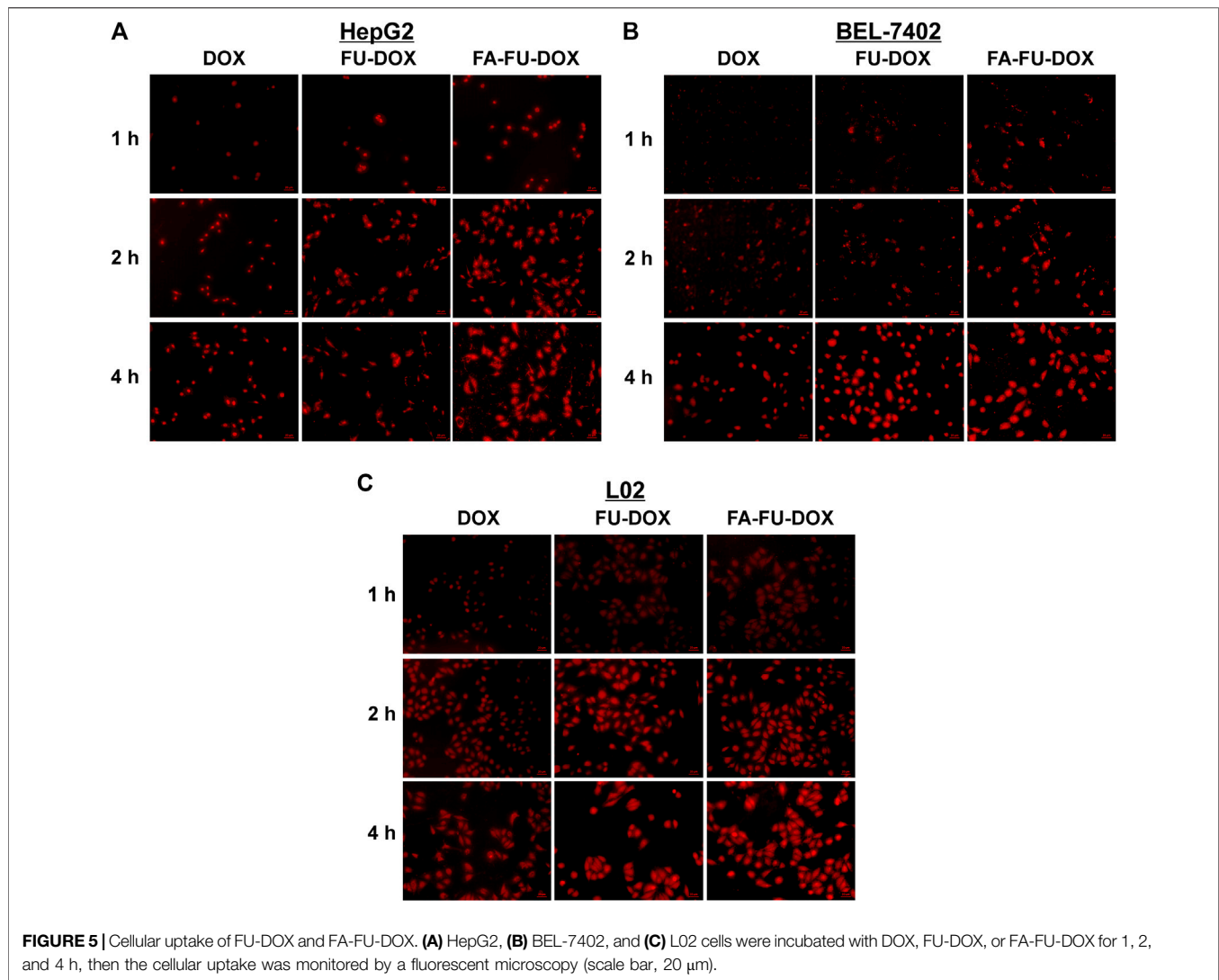

FIGURE 4 | The cumulative release kinetics of DOX from FU-DOX and FA-FU-DOX in PBS at a pH of 7.4 or 5.9 at 37°C.

FIGURE 5 | Cellular uptake of FU-DOX and FA-FU-DOX. **(A)** HepG2, **(B)** BEL-7402, and **(C)** L02 cells were incubated with DOX, FU-DOX, or FA-FU-DOX for 1, 2, and 4 h, then the cellular uptake was monitored by a fluorescent microscopy (scale bar, 20 μm).

RESULTS

Preparation and Characterization of FA-FU-DOX

As shown in **Figure 1**, FA-FU-DOX was successfully synthesized and characterized using NMR spectroscopy. The NMR spectrum of FA-FU-DOX (**Figure 2**) showed signals at 8.64, 7.64, 6.94, 6.65, 4.48, and 4.33 ppm, representing H-carbon units of FA, and signals at 7.90, 5.47, 5.30, 4.94, 4.85, 4.57, 4.20, and 3.98 ppm, belonging to H-carbon units of DOX, which indicated that FA and DOX had been successfully linked to FU carrier. The formation of FA-FU-DOX was further validated by IR spectroscopy (**Supplementary Figure S1**). Except for the characteristic peaks belonging to DOX (1,615, 1,584, 1,283, 1,211, and 1,115 cm^{-1}), FA (1,512 and 1,407 cm^{-1}), and FU (1,380 and 1,081 cm^{-1}) in the IR spectrum of FA-FU-DOX, the absence of the carbonyl peak of DOX at 1730 cm^{-1} and the presence of the -C=N peak of the hydrazone bond at

1,638 cm^{-1} were observed, indicating the successful coupling of the carbonyl group of DOX with the amine group of FU-CONHNH2. The large endothermic peak at 67°C in the DSC spectrum of FA-FU-DOX also confirmed the formation of this conjugate (**Supplementary Figure S2**).

The TEM images of FU, FU-DOX, and FA-FU-DOX are shown in **Figure 3**. Compared to FU, FU-DOX and FA-FU-DOX were larger in diameters, indicating the coupling of DOX and/or FA with FU. DLS established that the mean diameters for FU-DOX and FA-FU-DOX conjugates were about 199 nm (PDI = 0.123) and 195 nm (PDI = 0.108), respectively. The diameters are suitable for efficient targeting in circulation.

Drug Release Study of FA-FU-DOX

The stabilities of FU-DOX and FA-FU-DOX were examined by evaluating the cumulative release of DOX at physiological (pH 7.4) and endolysosomal pH conditions (pH 5.9). As shown in **Figure 4**, after 96 h of incubation, the cumulative
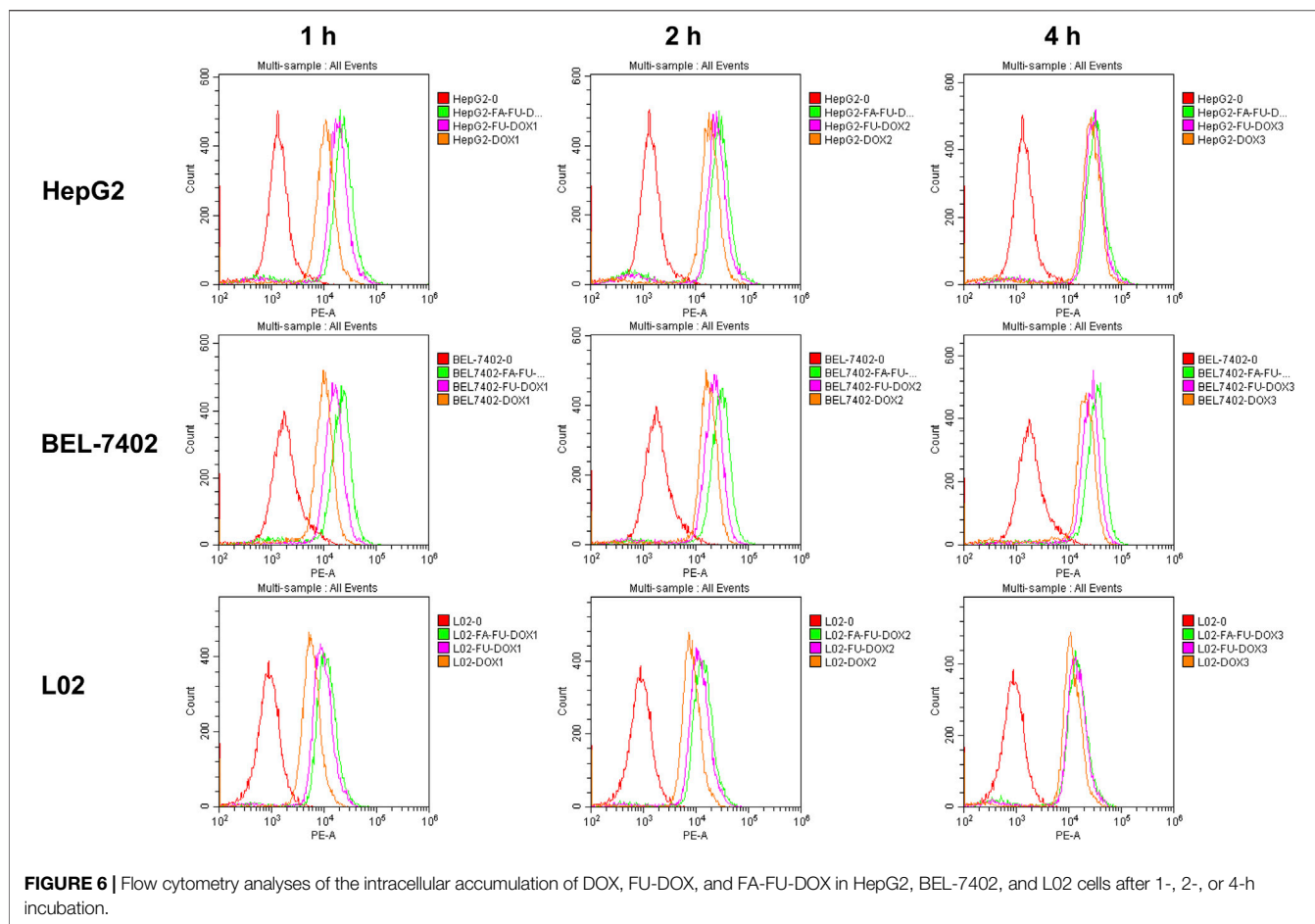
FIGURE 6 | Flow cytometry analyses of the intracellular accumulation of DOX, FU-DOX, and FA-FU-DOX in HepG2, BEL-7402, and L02 cells after 1-, 2-, or 4-h incubation.

release rates of DOX from FA-FU-DOX were found to be 32% (pH 7.4) and 42% (pH 5.9), respectively, while that from FU-DOX were 34% (pH 7.4) and 41% (pH 5.9), respectively. These results were consistent with the degradation characteristics of the hydrazone bond. The introduction of FA did not significantly alter the release kinetics. Both FU-DOX and FA-FU-DOX are expected to release DOX more rapidly in cancer cells after endocytosis than in circulation (Gao et al., 2017).

Cellular Uptake of FA-FU-DOX

The cellular uptake of DOX, FU-DOX, and FA-FU-DOX was investigated in the HCC cell lines BEL-7402 (FR-positive) (Dai et al., 2011) and HepG2 (FR-negative) (Gao et al., 2015) and the normal human hepatocytes L02 (FR-negative). As shown in **Figure 5**, the fluorescence microscopy images exhibited that DOX, FU-DOX, and FA-FU-DOX (shown as the red dots) were uptaken by all three cell lines in a time-dependent manner. The FU-DOX and FA-FU-DOX conjugates exhibited higher fluorescence intensity than free DOX, especially at 1 h incubation time, indicating a higher amount of cellular uptake than that for free DOX. It may be explained that the intracellular drug accumulation was efficiently promoted by the FU carrier at the experimental conditions (Grebinyk et al., 2019). Moreover, FA-FU-DOX showed the best cellular uptake in FR-positive

BEL-7402 cells but it did not exhibit significant higher accumulation than FU-DOX in FR-negative HepG2 and L02 cells (**Figure 5**), which suggested that the attachment of FA to FU-DOX enhanced the uptake of the conjugates into FR-positive cells via an FR-mediated endocytic process. Similar results were also obtained by flow cytometry analyses, confirming the important roles of FA and FU in enhancing the cellular uptake of DOX (**Figure 6**).

In Vitro Anticancer Activity of FA-FU-DOX

We further compared the *in vitro* anticancer activities of DOX, FU-DOX, and FA-FU-DOX in HepG2, BEL-7402, and L02 cell lines. As shown in **Figure 7**, all cell lines were more sensitive to DOX than FU-DOX or FA-FU-DOX, which could be attributed to the slow release of DOX from FU-DOX and FA-FU-DOX after endocytosis. Importantly, DOX did not show any selective cytotoxicity against cancer cells but exhibited more potent inhibitory effects on the viability of normal human hepatocytes L02. However, FU-DOX and FA-FU-DOX showed significantly weaker cytotoxicities against L02 cells, especially at lower concentrations (32 and 64 nM), suggesting that the conjugations of FU and FA to DOX could improve the safety profile of DOX. Furthermore, FA-FU-DOX exhibited more potent cytotoxicity than FU-DOX in FR-positive BEL-7402
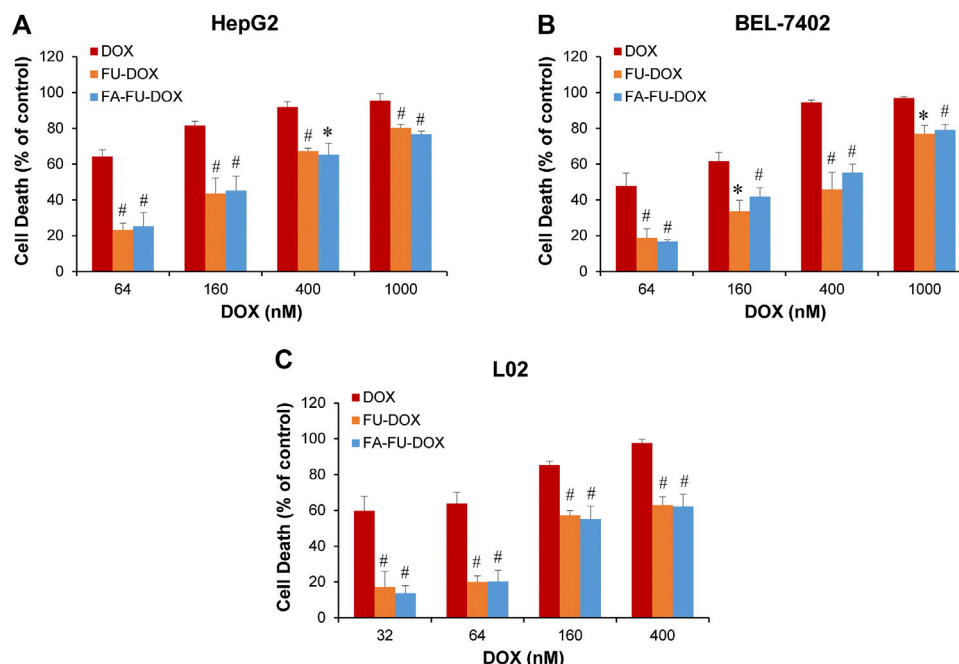
FIGURE 7 | *In vitro* cytotoxicity of DOX, FU-DOX, and FA-FU-DOX. **(A)** HepG2, **(B)** BEL-7402, and **(C)** L02 cells were exposed to various concentrations of DOX, FU-DOX, and FA-FU-DOX for 72 h for determination of cell death by CCK-8 assays. Data represent mean ± SD from three independent experiments (*$p < 0.05$ and #$p < 0.01$).

cells (at 160 and 400 nM), further supporting the inference of FA-mediated endocytosis and FU-mediated transportation.

CONCLUSION

In the present study, we designed, synthesized, and characterized the FA-FU-DOX conjugate as a new delivery system for the commonly used chemotherapeutic agent DOX. FA-FU-DOX has a diameter of around 190–200 nm, beneficial to the targeting of tumor tissues in the circulation. Our results have shown that the cumulative release rates of DOX from FU-DOX and FA-FU-DOX are similar at both physiological (pH 7.4) and endolysosomal pH conditions (pH 5.9), which is in line with the degradation features of the hydrazine group (Liu et al., 2014; Rezaian et al., 2018). We have also shown that FU-DOX and FA-FU-DOX have a higher release rate in an acidic environment, suggesting that DOX may release from these conjugates faster in the tumor microenvironment (acidic environment) (Seyfoori et al., 2019; Maleki et al., 2020).

Because FR is overexpressed in tumor tissues but restricted in normal tissues, it has been considered as a promising target for developing efficient TTDDSs. FA and methotrexate (MTX) through ethylenediamine have been attached to the surface of functionalized multi-walled carbon nanotubes by Karimi et al., which improves the cancer cell-targeting ability of MTX and enhances its anticancer activity (Karimi et al., 2019). Moreover, the modification of nanomaterials with FA

terminated-polyglycol as well as the subsequent loading with DOX improve the biocompatibility and selectivity against cancer cells, consequently improving its ability to eradicate tumors *in vivo* with negligible systemic toxicity (Wang et al., 2018). Besides, Yan *et al.* have used FA-modified multi-walled carbon nanotubes to deliver DOX to tumor sites, which not only enhanced the suppression of tumor growth but also decreased the side effects of DOX (Yan et al., 2018).

In this study, the cellular uptake and cytotoxicities of FU-DOX and FA-FU-DOX have been investigated in BEL-7402 (HCC, FR-positive), HepG2 (HCC, FR-negative), and L02 (normal, FR-negative) cells. It has been observed that the attachment of FA to FU-DOX increases the cellular uptake in FR-positive BEL-7402 cells in an FR-dependent manner. As expected, FA-FU-DOX has also exhibited more potent cytotoxicity than FU-DOX in BEL-7402 cells but not in FR-negative HepG2 and L02 cells. Besides, FU-DOX and FA-FU-DOX have shown relatively weak cytotoxicities against normal L02 cells. Taken together, the FA-FU-DOX conjugate has a better selectivity against cancer cells and a more promising safety profile.

In conclusion, our studies have demonstrated that the FA-FU-DOX conjugate has the potential to be developed as an effective approach for enhancing the efficacy and reducing the toxicity of chemotherapeutic drugs. Further investigations are warranted to examine the tumor-targeting efficacy and safety in clinically relevant animal models, especially liver cancer models.

DATA AVAILABILITY STATEMENT

The raw data supporting the conclusions of this article will be made available by the authors, without undue reservation.

AUTHOR CONTRIBUTIONS

BX, LY, YH, and ZX designed and conducted experiments, and wrote the manuscript. JJQ and XDC organized, conceived, and supervised the study. All authors read and approved the manuscript.

FUNDING

ACKNOWLEDGMENTS

SUPPLEMENTARY MATERIAL

The Supplementary Material for this article can be found online at: https://www.frontiersin.org/articles/10.3389/fphar.2020.598155/full#supplementary-material.

REFERENCES

Borović, M. L., Ičević, I., Kanački, Z., Žikić, D., Seke, M., Injac, R., et al. (2014). Effects of fullerenol C60(OH)24 nanoparticles on a single-dose doxorubicin-induced cardiotoxicity in pigs: an ultrastructural study. *Ultrastruct. Pathol.* 38 (2), 150–163. doi:10.3109/01913123.2013.822045

Boss, S. D., and Ametamey, S. M. (2020). Chaudhuri, S. D., and Ametamey, S. M. (2020). Development of folate receptor–targeted PET radiopharmaceuticals for tumor imaging-A bench-tobedside journey. *Cancers* 12 (6), 1508. doi:10.3390/cancers12061508

Chaudhuri, P., Paraskar, A., Soni, S., Mashelkar, R. A., and Sengupta, S. (2009). Fullerenol–cytotoxic conjugates for cancer chemotherapy. *ACS Nano.* 3 (9), 2505–2514. doi:10.1021/nn900318y

Dai, J., Zou, S., Pei, Y., Cheng, D., Ai, H., and Shuai, X. (2011). Polyethylenimine-grafted copolymer of poly(l-lysine) and poly(ethylene glycol) for gene delivery. *Biomaterials* 32 (6), 1694–1705. doi:10.1016/j.biomaterials.2010.10.044

Elshater, A.-E. A., Haridy, M. A. M., Salman, M. M. A., Fayyad, A. S., and Hammad, S. (2018). Fullerene C60 nanoparticles ameliorated cyclophosphamide-induced acute hepatotoxicity in rats. *Biomed. Pharmacother.* 97, 53–59. doi:10.1016/j.biopha.2017.10.134

Fernández, M., Javaid, F., and Chudasama, V. (2018). Advances in targeting the folate receptor in the treatment/imaging of cancers. *Chem. Sci.* 9 (4), 790–810. doi:10.1039/c7sc04004k

Gao, W., Ye, G., Duan, X., Yang, X., and Yang, V. C. (2017). Transferrin receptor-targeted pH-sensitive micellar system for diminution of drug resistance and targetable delivery in multidrug-resistant breast cancer. *Ijn* Vol. 12, 1047–1064. doi:10.2147/IJN.S115215

Gao, Y., Li, Z., Xie, X., Wang, C., You, J., Mo, F., et al. (2015). Dendrimeric anticancer prodrugs for targeted delivery of ursolic acid to folate receptor-expressing cancer cells: synthesis and biological evaluation. *Eur. J. Pharmaceut. Sci.* 70, 55–63. doi:10.1016/j.ejps.2015.01.007

Gonçalves, M., Mignani, S., Rodrigues, J., and Tomás, H. (2020). A glance over doxorubicin based-nanotherapeutics: From proof-of-concept studies to solutions in the market. *J. Contr.ournal of Controlled Release* 317, 347–374. doi:10.1016/j.jconrel.2019.11.016

Grebinyk, A., Prylutska, S., Chepurna, O., Grebinyk, S., Prylutskyy, Y., Ritter, U., et al. (2019). Synergy of chemo- and photodynamic therapies with C60 fullerene-doxorubicin nanocomplex. *Nanomaterials* 9 (11), 1540. doi:10.3390/nano9111540

Hao, T., Li, J., Yao, F., Dong, D., Wang, Y., Yang, B., et al. (2017). Injectable fullerenol/alginate hydrogel for suppression of oxidative stress damage in brown adipose-derived stem cells and cardiac repair. *ACS Nano.* 11 (6), 5474–5488. doi:10.1021/acsnano.7b00221

Kalyanaraman, B. (2020). Teaching the basics of the mechanism of doxorubicin-induced cardiotoxicity: Have we been barking up the wrong tree? *Redox Biology* 29, 101394. doi:10.1016/j.redox.2019.101394

Karimi, A., Erfan, M., Mortazavi, S. A., Ghorbani-Bidkorbeh, F., Kobarfard, F., and Shirazi, F. H. (2019). Functionalisation of carbon nanotubes by methotrexate and study of synchronous photothermal effect of carbon nanotube and anticancer drug on cancer cell death. *IET Nanobiotechnol.* 13 (1), 52–57. doi:10.1049/iet-nbt.2018.5085

Kazemzadeh, H., and Mozafari, M. (2019). Fullerene-based delivery systems. *Drug Discov. Today* 24 (3), 898–905. doi:10.1016/j.drudis.2019.01.013

Kepinska, M., Kizek, R., and Milnerowicz, H. (2018a). Fullerene as a doxorubicin nanotransporter for targeted breast cancer therapy: capillary electrophoresis analysis. *Electrophoresis* 39 (18), 2370–2379. doi:10.1002/elps.201800148

Kepinska, M., Kizek, R., and Milnerowicz, H. (2018b). Metallothionein and superoxide dismutase-antioxidative protein status in fllerene-doxorubicin delivery to MCF-7 human breast cancer cells. *Ijms* 19 (10), 3253. doi:10.3390/ijms19103253

Kumar, M., and Raza, K. (2018). C60-fullerenes as drug delivery carriers for anticancer agents: promises and hurdles. *Pnt* 5 (3), 169–179. doi:10.2174/2211738505666170301142232

Li, X., Yang, X., Liu, Y., Gong, N., Yao, W., Chen, P., et al. (2013). Japonicone A suppresses growth of Burkitt lymphoma cells through its effect on NF- B. *Clin. Canc. Res.* 19 (11), 2917–2928. doi:10.1158/1078-0432.ccr-12-3258

Maleki, R., Khoshoei, A., Ghasemy, E., and Rashidi, A. (2020). Molecular insight into the smart functionalized TMC-Fullerene nanocarrier in the pH-responsive adsorption and release of anti-cancer drugs. *J. Mol. Graph. Model.* 100, 107660. doi:10.1016/j.jmgm.2020.107660

Martinez, Z. S., Castro, E., Seong, C.-S., Cerón, M. R., Echegoyen, L., and Llano, M. (2016). Fullerene derivatives strongly inhibit HIV-1 replication by affecting virus maturation without impairing protease activity. *Antimicrob. Agents Chemother.* 60 (10), 5731–5741. doi:10.1128/aac.00341-16

Ohulchanskyy, A., Prylutska, S., Grebinyk, S., Prylutskyy, Y., Ritter, U., Matyshevska, O., et al. (2019). Complexation with C60 fullerene increases doxorubicin efficiency against leukemic cells in vitro. *Nanoscale Res. Lett.* 14 (1), 61. doi:10.1186/s11671-019-2894-1

Ouyang, C., Zhang, S., Xue, C., Yu, X., Xu, H., Wang, Z., et al. (2020). Precision-guided missile-like DNA nanostructure containing warhead and guidance control for aptamer-based targeted drug delivery into cancer cells *in vitro* and *in vivo*. *J. Am. Chem. Soc.* 142 (3), 1265–1277. doi:10.1021/jacs.9b09782

Petrovic, D., Seke, M., Borovic, M. L., Jovic, D., Borisev, l., Srdjenovic, B., et al. (2018). Hepatoprotective effect of fullerenol/doxorubicin nanocomposite in

acute treatment of healthy rats. *Exp. Mol. Pathol.* 104 (3), 199–211. doi:10.1016/jyexmp.2018.04.005

Qin, J.-J., Jin, H.-Z., Huang, Y., Zhang, S.-D., Shan, L., Voruganti, S., et al. (2013). Selective cytotoxicity, inhibition of cell cycle progression, and induction of apoptosis in human breast cancer cells by sesquiterpenoids from Inula lineariifolia Turcz. *Eur. J. Med. Chem.* 68, 473–481. doi:10.1016/j.ejmech.2013.07.018

Qin, J.-J., Wang, W., Sarkar, S., and Zhang, R. (2016). Oral delivery of anti-MDM2 inhibitor SP141-loaded FcRn-targeted nanoparticles to treat breast cancer and metastasis. *J. Contr. Release* 237, 101–114. doi:10.1016/j.jconrel.2016.07.008

Qin, L., Yu, M., Zhang, Y., Wang, C., and Lu, H. (2014). Hydrazide functionalized core-shell magnetic nanocomposites for highly specific enrichment of N-glycopeptides. *ACS Appl. Mater. Interfaces* 6 (10), 7823–7832. doi:10.1021/am501110e

Raj, S., Khurana, S., Choudhari, R., Kesari, K. K., Kamal, M. A., Garg, N., et al. (2019). Specific targeting cancer cells with nanoparticles and drug delivery in cancer therapy. *Semin. Canc. Biol.* doi:10.1016/j.semcancer.2019.11.002

Ruokolainen, M., Maleki, R., Dahri Dahroud, M., Alamdari, A., and Alimohammadi, M. (2018). pH-sensitive co-adsorption/release of doxorubicin and paclitaxel by carbon nanotube, fullerene, and graphene oxide in combination with N-isopropylacrylamide: a molecular dynamics study. *Biomolecules* 8 (4), 127. doi:10.3390/biom8040127

Seke, M., Petrovic, D., Djordjevic, A., Jovic, D., Borovic, M. L., Kanacki, Z., et al. (2016). Fullerenol/doxorubicin nanocomposite mitigates acute oxidative stress and modulates apoptosis in myocardial tissue. *Nanotechnology* 27 (48), 485101. doi:10.1088/0957-4484/27/48/485101

Seyfoori, A., Sarfarazijami, S., and Seyyed Ebrahimi, S. A. (2019). pH-responsive carbon nanotube-based hybrid nanogels as the smart anticancer drug carrier. *Artif. Cells, Nanomed. Biotechnol.* 47 (1), 1437–1443. doi:10.1080/21691401.2019.1596939

Su, M., Xie, J., Zeng, Q., Shu, M., Liu, J., and Jiang, Z. (2020). Enzymatic synthesis of PEGylated lactide-diester-diol copolyesters for highly efficient targeted anticancer drug delivery. *Mater. Sci. Eng. C* 115, 111125. doi:10.1016/j.msec.2020.111125

Tan, Y. Y., Yap, P. K., Xin Lim, G. L., Mehta, M., Chan, Y., Ng, S. W., et al. (2020). Perspectives and advancements in the design of nanomaterials for targeted cancer theranostics. *Chem. Biol. Interact.* 329, 109221. doi:10.1016/j.cbi.2020.109221

Tie, Y., Zheng, H., He, Z., Yang, J., Shao, B., Liu, L., et al. (2020). Targeting folate receptor β positive tumor-associated macrophages in lung cancer with a folate-modified liposomal complex. *Sig. Transduct. Target Ther.* 5 (1), 6. doi:10.1038/s41392-020-0115-0

Voruganti, S., Qin, J.-J., Sarkar, S., Nag, S., Walbi, I. A., Wang, S., et al. (2015). Oral nanodelivery of anticancer ginsenoside 25-OCH3-PPD, a natural inhibitor of the MDM2 oncogene: nanoparticle preparation, characterization,in vitroandin vivoanti-prostate cancer activity, and mechanisms of action. *Oncotarget* 6 (25), 21379–21394. doi:10.18632/oncotarget.4091

Wang, D., Meng, L., Fei, Z., Hou, C., Long, J., Zeng, L., et al. (2018). Multi-layered tumor-targeting photothermal-doxorubicin releasing nanotubes eradicate tumors in vivo with negligible systemic toxicity. *Nanoscale* 10 (18), 8536–8546. doi:10.1039/c8nr00663f

Wang, V., Djordjevic, A., Srdjenovic, B., Milic-Tores, V., Segrt, Z., Dragojevic-Simic, V., et al. (2017). Fullerenol nanoparticles prevents doxorubicin-induced acute hepatotoxicity in rats. *Exp. Mol. Pathol.* 102 (2), 360–369. doi:10.1016/j.yexmp.2017.03.005

Wang, W., Cheng, J.-W, Qin, J.-J., Hu, B., Li, X., Nijampatnam, B., et al. (2019). MDM2-NFAT1 dual inhibitor, MA242: effective against hepatocellular carcinoma, independent of p53. *Canc. Lett.* 459, 156–167. doi:10.1016/j.jcanlet.2019.114429

Wang, W., Yang, J., Liao, Y.-Y., Cheng, G., Chen, J., Cheng, X.-D., et al. (2020a). Cytotoxic nitrogenated azaphilones from the deep-sea-derived fungus chaetomium globosum MP4-S01-7. *J. Nat. Prod.* 83 (4), 1157–1166. doi:10.1021/acs.jnatprod.9b01165

Wang, W., Yang, J., Liao, Y.-Y., Cheng, G., Chen, J., Mo, S., et al. (2020b). Aspeterreurone A, a cytotoxic dihydrobenzofuran-phenyl acrylate hybrid from the deep-sea-derived fungus aspergillus terreus CC-S06-18. *J. Nat. Prod.* 83 (6), 1998–2003. doi:10.1021/acs.jnatprod.0c00189

Xiao, H., Guo, Y., Liu, H., Liu, Y., Wang, Y., Li, C., et al. (2020). Structure-based design of charge-conversional drug self-delivery systems for better targeted cancer therapy. *Biomaterials* 232, 119701. doi:10.1016/j.biomaterials.2019.119701

Xu, J., Wang, H., Hu, Y., Zhang, Y. S, Wen, L., Yin, F., et al. (2019). Inhibition of CaMKIIα activity enhances antitumor effect of fullerene C60 nanocrystals by suppression of autophagic degradation. *Adv. Sci.* 6 (8), 1801233. doi:10.1002/advs.201801233

Xu, Y., Zhu, J., Xiang, K., Li, Y., Sun, R., Ma, J., et al. (2011). Synthesis and immunomodulatory activity of [60]fullerene-tuftsin conjugates. *Biomaterials* 32 (36), 9940–9949. doi:10.1016/j.biomaterials.2011.09.022

Yan, Y., Wang, R., Hu, Y., Sun, R., Song, T., Shi, X., et al. (2018). Stacking of doxorubicin on folic acid-targeted multiwalled carbon nanotubes for in vivo chemotherapy of tumors. *Drug Deliv.* 25 (1), 1607–1616. doi:10.1080/10717544.2018.1501120

Zhang, J., Wang, W., Zhou, Y., Yang, J., Xu, J., Xu, Z., et al. (2020). Terphenyllin suppresses orthotopic pancreatic tumor growth and prevents metastasis in mice. *Front. Pharmacol.* 11, 457. doi:10.3389/fphar.2020.00457